Cylindrical Rotating Triboelectric Nanogenerator

Peng Bai,[†,‡,⊥] Guang Zhu,[†,⊥] Ying Liu,[†] Jun Chen,[†] Qingshen Jing,[†] Weiqing Yang,[†] Jusheng Ma,[‡] Gong Zhang,[‡] and Zhong Lin Wang[†,§,*]

[†]School of Materials Science and Engineering, Georgia Institute of Technology, Atlanta, Georgia 30332-0245, United States, [‡]Department of Mechanical Engineering, Tsinghua University, Beijing 100084, China, and [§]Beijing Institute of Nanoenergy and Nanosystems, Chinese Academy of Sciences, Beijing 100083, China. [⊥]These authors contributed equally.

ABSTRACT We demonstrate a cylindrical rotating triboelectric nanogenerator (TENG) based on sliding electrification for harvesting mechanical energy from rotational motion. The rotating TENG is based on a core–shell structure that is made of distinctly different triboelectric materials with alternative strip structures on the surface. The charge transfer is strengthened with the formation of polymer nanoparticles on surfaces. During coaxial rotation, a contact-induced electrification and the relative sliding between the contact surfaces of the core and the shell result in an "in-plane" lateral polarization, which drives the flow of electrons in the external load. A power density of 36.9 W/m^2 (short-circuit current of 90 μA and open-circuit voltage of 410 V) has been achieved by a rotating TENG with 8 strip units at a linear rotational velocity of 1.33 m/s (a rotation rate of 1000 r/min). The output can be further enhanced by integrating more strip units and/or applying larger linear rotational velocity. This rotating TENG can be used as a direct power source to drive small electronics, such as LED bulbs. This study proves the possibility to harvest mechanical energy by TENGs from rotational motion, demonstrating its potential for harvesting the flow energy of air or water for applications such as self-powered environmental sensors and wildlife tracking devices.

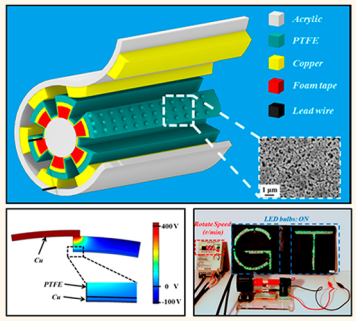

KEYWORDS: triboelectric nanogenerators · rotation · energy harvesting

As a type of contact electrification in which a material becomes electrically charged after contacting with a different material, triboelectric effect is one of the most universal phenomena and is responsible for generating most everyday static electricity that usually leads to undesirable consequences, such as potential hazard to delicate electronics and public safety.[1−6] Though it has been known for centuries, it is still an under explored effect with the mechanism in debate.[7−12] Recently, this effect was successfully used as an effective means for harvesting mechanical energy, leading to the invention of the triboelectric nanogenerators (TENGs).[13,14] Utilizing the triboelectric effect that couples with electrostatic induction,[15,16] the TENG offers a simple, reliable, cost-effective, and efficient method to harvest mechanical energy for self-powered applications without reliance on traditional power supplies. Demonstrated applications include micropatterning,[17] powering portable electronics,[18−20] and self-powered sensors.[21,22]

Two basic operating principles of the TENG have been developed, that is, contact mode and sliding mode. For the contact mode, it relies on repeated contact and separation between two materials that have different triboelectric polarities. Such an operating principle introduces a changing gap in the TENG, making it difficult for device sealing and packaging and thus limiting the TENG's applications in harsh environment. More recently, sliding mode based on lateral electrification has been reported.[23,24] Relative displacement between two contact surfaces of different triboelectric polarities creates uncompensated triboelectric charges that drive induced free electrons to flow through the external circuit. The newly developed sliding mode greatly expands the TENGs' applicability to harvest energy from continuous motion and makes it possible for a fully packaged device.

Here, in this work, a coaxial cylindrical structured rotating TENG is developed to harvest mechanical energy from rotation analogous to an electromagnetic induction-based generator. A TENG with a total contact area of 12 cm^2 contains multiple strip units that are connected in parallel. The instantaneous short-circuit current (I_{sc})

* Address correspondence to zlwang@gatech.edu.

Received for review May 16, 2013 and accepted June 21, 2013.

Published online June 25, 2013
10.1021/nn402491y

and the open-circuit voltage (V_{oc}) could reach 90 μA and 410 V, respectively, for a TENG with 8 strip units at a linear rotational velocity of 1.33 m/s, corresponding to an instantaneous maximum power density of 36.9 W/m^2 and an equivalent average direct current of 45.6 μA. Higher output power can be achieved by using a higher density of strip units and/or applying larger linear rotational velocity. At a linear rotational velocity of 1.33 m/s, the TENG can be used as a direct power source for simultaneously powering 90 commercial light-emitting diode (LED) bulbs in real time. Since rotation is one of the most common forms of motion in ambient environment, a fully packaged cylindrical rotating TENG has potential applications in harsh environment, outdoors or even under water, to harvest energy from water flow.

RESULTS AND DISCUSSION

A schematic diagram of a rotating TENG with 6 strip units is shown in Figure 1a. The TENG has a core–shell structure that is composed of a column connected to a rotational motor and a hollow tube fixed on a holder. Here, acrylic was selected as the structural material due to its light weight, good machinability, and proper strength. On the inner surface of the fixed tube, metal strips made of copper are evenly distributed with each having a central angle of 30°, creating equal-sized intervals between. These metal strips, connected by a bus at one end, play dual roles as a sliding surface and as a common electrode. On the surface of the rotatable column, a collection of separated strips of foam tape was adhered as a buffer layer with a central angle of 30° for each unit. The buffer layer is a critical design that ensures robustness and tolerance on off-axis rotation, which will be discussed in details later. On top of the foam tape, a layer of copper and a layer of polytetrafluoroethylene (PTFE) film are conformably attached in sequence. The copper layer serves as the back electrode of the TENG. The outer surface of the PTFE film is modified by spreading a layer of PTFE nanoparticles for enhancing energy conversion efficiency. PTFE nanoparticles with an average diameter of 100 nm spread uniformly on the surface of PTFE film as shown in Figure 1b. As demonstrated in Figure 1a, the PTFE film on the column and the metal strips on the tube were configured to match for a full contact during rotation. These two components and the motor are set to be coaxial to minimize wobbling during rotation. Further details of the fabrication process will be discussed in the Experimental Section.

The working principle of a rotating TENG can be described by the coupling of contact electrification and electrostatic induction. The design of the cylindrical rotating TENG is based on the relative sliding motion of grated surfaces. Here, a pair of sliding units is selected to illustrate the process of electricity generation, as schemed in Figure 2. The foam tape and

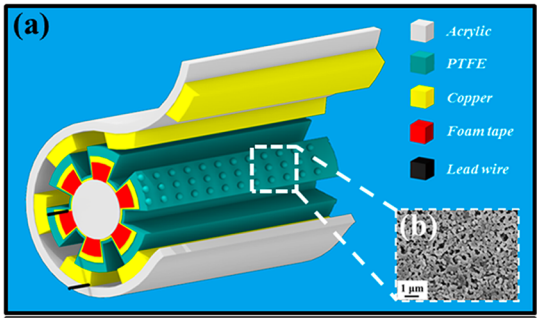

Figure 1. (a) Schematic of the rotating TENG with 6 strip units. (b) SEM image of PTFE nanoparticles on the surface of PTFE film.

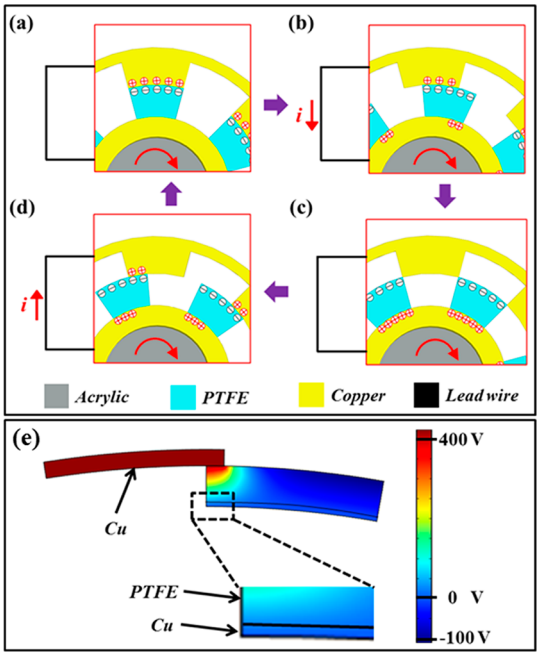

Figure 2. Working principle of the rotating TENG. Distributions of charges at (a) fully aligned position, (b) two surfaces are sliding apart, (c) fully mismatched position, and (d) two surfaces are sliding back together. (e) COMSOL simulation result of the electric potential distribution when the two surfaces are sliding apart (a constant value of triboelectric charge density of 3.89 × 10^{-6} C/m^2, and electric potential of the back electrode is set to be zero).

nanoparticles on the PTFE film are not presented for simplification and clear illustration. At the aligned position, the two parts of the sliding pair completely match because of the same central angle. Upon contact between the PTFE film and the metal strips, charge transfer takes place. Due to the difference on triboelectric polarities,[25] electrons are injected from metal into the surface of PTFE. Since the two sliding surfaces are completely aligned, triboelectric charges with opposite polarities are fully balanced out, making no electron flow in the external circuit (Figure 2a). Once a relative sliding occurs as a result of rotation, triboelectric charges on the mismatched areas cannot be compensated. The negative ones on the PTFE will drive free electrons on the back electrode to the sliding

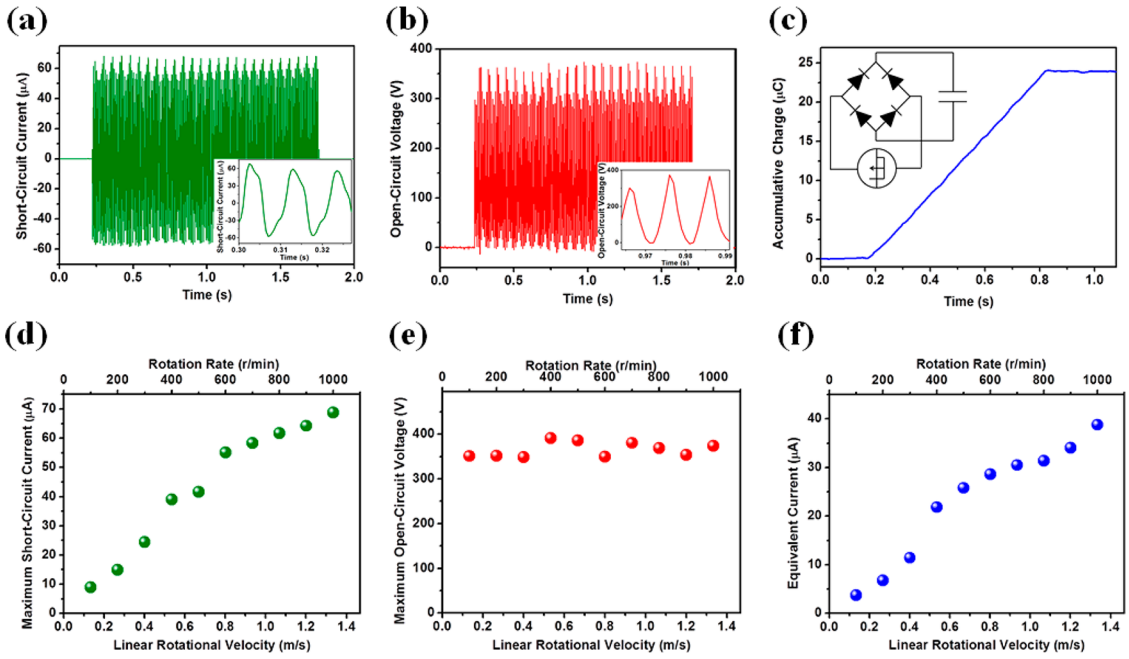

Figure 3. Electricity output of a rotating TENG with 6 strip units. (a) I_{sc} of a rotating TENG at a linear rotational velocity of 1.33 m/s (a rotation rate of 1000 r/min). Inset: enlarged view of the current peaks. (b) V_{oc} of a rotating TENG at a linear rotational velocity of 1.33 m/s (a rotation rate of 1000 r/min). Inset: enlarged view of the voltage peaks. (c) Accumulative inductive charges generated by a rotating TENG. Inset: electric circuit diagram. (d) Maximum I_{sc} as a function of linear rotational velocity/rotation rate. (e) Maximum V_{oc} as a function of linear rotational velocity/rotation rate. (f) Equivalent direct current as a function of linear rotational velocity/rotation rate.

electrode through the external circuit due to electrostatic induction, neutralizing positive triboelectric charges on the sliding electrode and leaving positive induced charges behind on the back electrode (Figure 2b). The flow of the induced electrons lasts until the mismatch between the two sliding surfaces reaches the maximum when the positive triboelectric charges are fully screened by induced electrons (Figure 2c). As the relative rotation continues, the PTFE film will come into contact with an adjacent metal strip (Figure 2d). Thus, the induced electrons will flow back in an opposite direction until the fully aligned position is restored (Figure 2a). Therefore, in a cycle of electricity generation process, AC electric output is generated. Since all of the sliding units are electrically connected in parallel, output current from different units are synchronized to constructively add up. As shown in Figure 2e, a simulation plot *via* COMSOL presents electric potential difference between the two electrodes in open-circuit condition when the pair of sliding parts are mismatched (a constant value of triboelectric charge density of 3.89×10^{-6} C/m^2, and electric potential of the back electrode is set to be zero).

To characterize the electric output, I_{sc} and V_{oc} of a rotating TENG with 6 strip units were measured at a rotation rate of 1000 r/min, corresponding to an equivalent linear rotational velocity of 1.33 m/s. As shown in Figure 3a, I_{sc} of 60 μA was achieved. An enlarged view in the inset exhibits continuous AC output current with a frequency of 100 Hz. The frequency is consistent with the one derived from the aforementioned working principle. The V_{oc} reached a maximum value of 373 V (Figure 3b), and the enlarged view in the inset of Figure 3b shows the oscillating behavior between zero and the peak value at a frequency that is the same as the output current. With a diode bridge (as inserted in Figure 3c), output current of different directions can be added up constructively, leading to accumulative induced charges. As illustrated in Figure 3c, the accumulative charges can reach 24.5 μC in 0.63 s, which corresponds to an effective direct current of 38.9 μA. To investigate the influence of rotation rate on the output of the rotating TENG, I_{sc} and V_{oc} at different rotation rates were measured. At a rotation rate of 100 r/min (a linear rotational velocity of 0.13 m/s), the amplitude of the AC current generated by a rotating TENG with 6 strip units is 9.0 μA. When the rotation rate increases to 1000 r/min (a linear rotational velocity of 1.33 m/s), the amplitude reaches 68.8 μA. An approximately linear relationship between the linear rotational velocity and the current amplitude can be derived from the results shown in Figure 3d. The linear relationship between the velocity and output current can be explained by the increasing frequency. Because the linear rotational velocity has no influence on the transferred charge density under constant displacement, a higher linear rotational velocity results in a faster charge transfer rate.

$$I = \frac{dq}{dt} = \frac{dq}{dl} \cdot v \qquad (1)$$

where q is the quantity of the triboelectric charges on one sliding surface; t is the time needed for charge transfer, which is the time needed for achieving the mismatched displacement; l is the mismatched displacement between the two sliding surfaces; v is the linear rotational velocity. Thus, an increased I_{sc} is expected. However, the V_{oc} stays stable at different rotation rate because the voltage is only a function of percentage of mismatch, as shown in Figure 3e (Supporting Information). For output charge, a higher current frequency produces a larger amount of accumulative charges within the same period of time, resulting in a larger equivalent direct current. As shown in Figure 3f, the equivalent direct current increases from 3.7 to 38.9 μA when the linear rotational velocity increases from 0.13 to 1.33 m/s.

It is to be noted that the density of sliding units in the rotating TENG is a critical factor that directly determines the electric output. As shown in Figure 4a, at a constant rotation rate of 1000 r/min, the output current is solely determined by the density of the sliding units. Though the total amount of induced charges transported between the two electrodes remains constant for a sliding distance of a unit, the frequency of the charge flow linearly depends on the number of the sliding units.[23] An enhancement on I_{sc} from 13.5 to 89.9 μA was achieved by increasing the number of sliding units from one to eight. Besides, similar enhancement could also be realized for output charge from 3.6 to 25 μC in 0.55 s (Figure 4c), which corresponds to equivalent DC output from 7.0 to 45.6 μA as inserted in Figure 4c. Because the length of strip units is much bigger than the thickness of the PTFE film, the density of sliding units has little influence on the amplitude of V_{oc} which stays stable around 360 V (Figure 4b).[23] However, the oscillation frequency of the voltage signal increases from 16.7 to 133.3 Hz. For a TENG with 8 sliding units, the instantaneous I_{sc} and V_{oc} could reach 90 μA and 410 V, respectively, at a linear rotational velocity of 1.33 m/s (a rotation rate of 1000 r/min), corresponding to an instantaneous power density of 36.9 W/m^2. It is expected that a higher electric output can be achieved if more units are fabricated in the rotating TENG. Moreover, the robustness of the TENG was investigated by long time operation of the TENG at a rotation rate of 1000 r/min. As shown in Figure 5a, after 20 000 rounds of operation, only a slight decline around 1.0% (from 68.81 to 68.09 μA) was observed for the amplitude of I_{sc} from a TENG with 6 units while the V_{oc} slightly dropped from 374 to 371 V (~0.7%). The minor decrease of the electric output can be explained by the deformation of the PTFE nanoparticles on the contact surfaces, the increased surface roughness of PTFE thin film, and the aggravation of off-axis rotation, which could reduce the effective contact area and lead to a decreased quantity of the triboelectric charges.

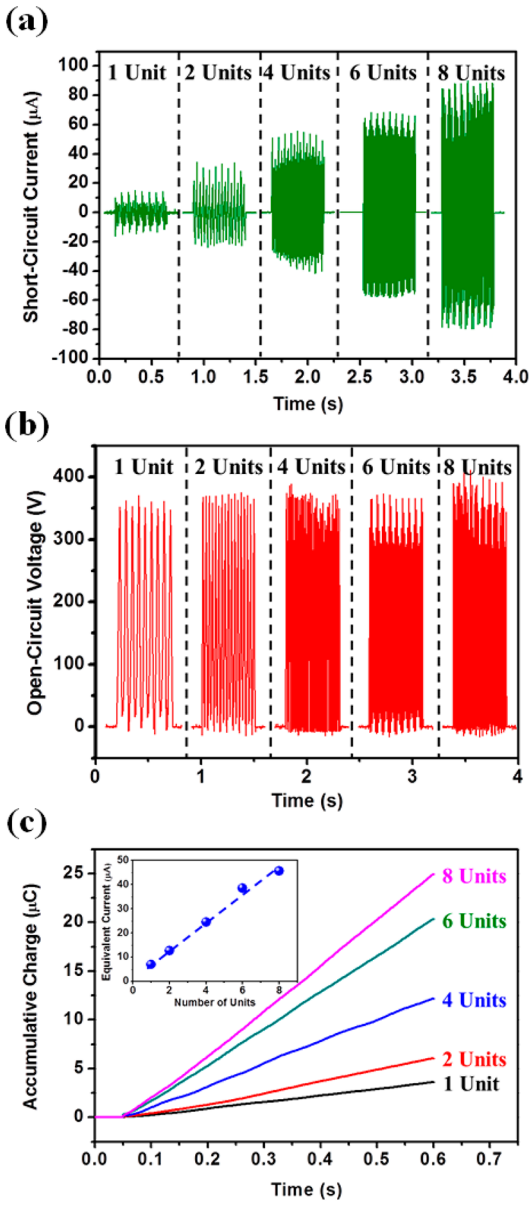

Figure 4. Electric output of a rotating TENG made of different strip units at a constant linear rotational velocity of 1.33 m/s (a rotation rate of 1000 r/min). (a) I_{sc} generated by rotating TENGs with multiple strip units. (b) V_{oc} generated by rotating TENGs with multiple strip units. (c) Accumulative inductive charges generated by rotating TENGs with multiple strip units. Inset: equivalent direct current as a function of number of strip units.

To demonstrate the ability of the rotating TENG as a direct power source for electronics, a total of 90 commercial LED bulbs were utilized as external loads (Figure 5b). They were divided into two groups, which were connected to a rotating TENG with reversed polarity. As illustrated in the circuit diagram in Figure 5c, 50 LED bulbs were connected in series, constituting the letter "G" on a circuit board shown in Figure 5b while the letter "T" consisted of another 40 LED bulbs connected in series with reversed polarity. As shown in Figure 5d, at a rotation rate of 722 r/min, the 90 LED bulbs could be powered by the TENG in real

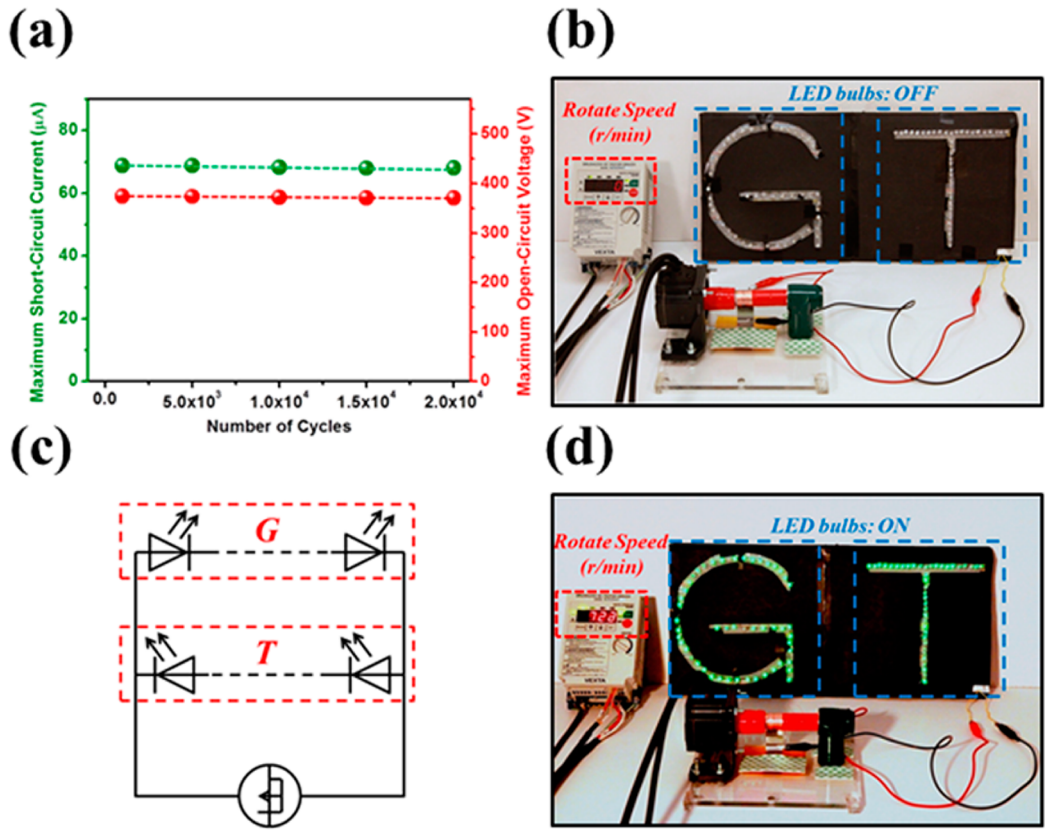

Figure 5. (a) Robustness of the rotating TENG. The electric output remains stable, although only a slight decline of the maximum I_{sc} and V_{oc} occurs. (b) Demonstration of the rotating TENG as a direct power source for driving 90 LED bulbs when the LED bulbs were off. (c) Electric circuit diagram, indicating that the two rows of LEDs are divided into two groups with reversed connection polarities, constituting the letters G and T, respectively. (d) Demonstration of the rotating TENG as a direct power source for driving 90 LED bulbs when the LED bulbs were on.

time. Due to the high frequency around 70 Hz of the output current, the 90 LED bulbs with reversed polarities could be continuously lighted up (see video in the Supporting Information).

CONCLUSIONS

In summary, we demonstrated a design of cylindrical rotating TENG based on sliding electrification. This rotating TENG provides an effective way to harvest mechanical energy from rotational motion. A TENG with 8 strip units on the surface could achieve a power density of 36.9 W/m^2 (I_{sc} of 90 μA and V_{oc} of 410 V) at a linear rotational velocity of 1.33 m/s (rotation rate of 1000 r/min). Higher output can be achieved if more strip units are fabricated in the TENG and/or a higher linear rotational velocity is applied. At a linear rotational velocity of 1.33 m/s, a rotating TENG can be used as a direct power source which can drive 90 commercial LED bulbs in real time. This study demonstrates the possibility to harvest mechanical energy by TENGs from rotational motion. It also can be used to design active sensors of rotational motion. With this unique design, fully packaged rotating TENGs can be further applied in harsh environment, outdoors, or under water to harvest energy from air and water flow. It is expected to be an effective power source for applications such as self-powered environmental sensors and wildlife tracking devices.

EXPERIMENTAL SECTION

Fabrication of a Rotating TENG with Multiple Strip Units. An acrylic column (diameter = 25.5 mm, length = 76 mm) and an acrylic hollow tube (internal diameter = 31.5 mm, external diameter = 33 mm, length = 38 mm) were used as the substrate. The size of the strip units was based on their quantity integrated in the TENG, and they were fabricated evenly with the same central angle. As an example, a unit has a size of 8.2 mm × 25.0 mm, 6 of them are fabricated in the TENG. Stuck on the surface of acrylic column, chemical-resistant polyethylene foam tape with a thickness of 3.175 mm was used as the buffer layer. PTFE thin films with a thickness of 25 μm were prepared and deposited with 100 nm of copper by magnetron sputtering. They were adhered onto the top of foam tape with the uncoated side exposed. Then, a 0.5 g sample of commercial PTFE dispersion in which the PTFE nanoparticles were dissolved in isopropyl alcohol was sprayed on the surface of PTFE thin films and dried in air. Grid copper electrodes (8.2 mm × 25.0 mm) with a thickness of 100 nm were deposited on a Kapton thin film (99 mm × 25.0 mm × 125 μm) by magnetron sputtering. Subsequently, the Kapton thin film was

adhered on the internal surface of the acrylic hollow tube at corresponding positions. The strip units were connected in parallel by external wiring.

Conflict of Interest: The authors declare no competing financial interest.

Acknowledgment. Research was supported by U.S. Department of Energy, Office of Basic Energy Sciences (Award DE-FG02-07ER46394), NSF (0946418), and the Knowledge Innovation Program of the Chinese Academy of Science (Grant No. KJCX2-YW-M13). P.B. thanks the support from the Chinese Scholars Council. Patents have been filed based on the research results presented in this manuscript.

Supporting Information Available: (1) Analytical model for calculating the maximum open-circuit voltage; (2) COMSOL simulation result of electric potential distribution; (3) enlarged view of short-circuit current of rotating TENGs with multiple working units; (4) supplementary video. This material is available free of charge *via* the Internet at http://pubs.acs.org.

REFERENCES AND NOTES

1. Pai, D. M.; Springett, B. E. Physics of Electrophotography. *Rev. Mod. Phys.* **1993**, *65*, 163–211.
2. Horn, R. G.; Smith, D. T. Contact Electrification and Adhesion between Dissimilar Material. *Science* **1992**, *256*, 362–364.
3. Liu, C.-Y.; Bard, A. J. Electrostatic Electrochemistry at Insulators. *Nat. Mater.* **2008**, *7*, 505–509.
4. Baytekin, B.; Baytekin, H. T.; Grzybowski, B. A. What Really Drives Chemical Reactions on Contact Charged Surfaces. *J. Am. Chem. Soc.* **2012**, *134*, 7223–7226.
5. Lowell, J.; Rose-Innes, A. C. Contact Electrification. *Adv. Phys.* **1980**, *29*, 947–1023.
6. Horn, R. G.; Smith, D. T.; Grabbe, A. Contact Electrification Induced by Monolayer Modification of a Surface and Relation to Acid−Base Interactions. *Nature* **1993**, *366*, 442–443.
7. Wiles, J. A.; Grzybowski, B. A.; Winkleman, A.; Whitesides, G. M. A Tool for Studying Contact Electrification in Systems Comprising Metals and Insulating Polymers. *Anal. Chem.* **2003**, *75*, 4859–4867.
8. Duke, C. B.; Fabish, T. J. Contact Electrification of Polymers: A Quantitative Model. *J. Appl. Phys.* **1978**, *49*, 315–321.
9. Soh, S.; Kwok, S. W.; Liu, H.; Whitesides, G. M. Contact De-electrification of Electrostatically Charged Polymers. *J. Am. Chem. Soc.* **2012**, *134*, 20151–20159.
10. Davies, D. K. Charge Generation on Dielectric Surfaces. *J. Phys. D: Appl. Phys.* **1969**, *2*, 1533–1537.
11. Diaz, A. F.; Guay, J. Contact Charging of Organic Materials: Ion *vs.* Electron Transfer. *IBM J. Res. Dev.* **1993**, *37*, 249–259.
12. McCarty, L. S.; Whitesides, G. M. Electrostatic Charging Due to Separation of Ions at Interfaces: Contact Electrification of Ionic Electrets. *Angew. Chem., Int. Ed.* **2008**, *47*, 2188–2207.
13. Wang, Z. L.; Zhu, G.; Yang, Y.; Wang, S. H.; Pan, C. F. Progress in Nanogenerators for Portable Electronics. *Mater.Today* **2012**, *15*, 532–543.
14. Fan, F.-R.; Tian, Z.-Q.; Wang, Z. L. Flexible Triboelectric Generator. *Nano Energy* **2012**, *1*, 328–334.
15. Fan, F.-R.; Lin, L.; Zhu, G.; Wu, W.; Zhang, R.; Wang, Z. L. Transparent Triboelectric Nanogenerators and Self-Powered Pressure Sensors Based on Micropatterned Plastic Films. *Nano Lett.* **2012**, *12*, 3109–3114.
16. Wang, S.; Lin, L.; Wang, Z. L. Nanoscale Triboelectric-Effect-Enabled Energy Conversion for Sustainably Powering Portable Electronics. *Nano Lett.* **2012**, *12*, 6339–6346.
17. Zhu, G.; Pan, C.; Guo, W.; Chen, C.-Y.; Yu, R.; Wang, Z. L. Triboelectric-Generator-Driven Pulse Electrodeposition for Micropatterning. *Nano Lett.* **2012**, *12*, 4960–4965.
18. Zhu, G.; Lin, Z.-H.; Jing, Q.; Bai, P.; Pan, C.; Yang, Y.; Zhou, Y.; Wang, Z. L. Toward Large-Scale Energy Harvesting by a Nanoparticle-Enhanced Triboelectric Nanogenerator. *Nano Lett.* **2013**, *13*, 847–853.
19. Bai, P.; Zhu, G.; Lin, Z.-H.; Jing, Q.; Chen, J.; Zhang, G.; Ma, J.; Wang, Z. L. Integrated Multilayered Triboelectric Nanogenerator for Harvesting Biomechanical Energy from Human Motion. *ACS Nano* **2013**, *7*, 3713–3719.
20. Yang, X.; Zhu, G.; Wang, S.; Zhang, R.; Lin, L.; Wu, W.; Wang, Z. L. A Self-Powered Electrochromic Device Driven by a Nanogenerator. *Energy Environ. Sci.* **2012**, *5*, 9462–9466.
21. Lin, Z.-H.; Zhu, G.; Zhou, Y.; Yang, Y.; Bai, P.; Chen, J.; Wang, Z. L. A Self-Powered Triboelectric Nanosensor for Mercury Ion Detection. *Angew. Chem.* **2013**, *19*, 5065–5069.
22. Yang, Y.; Lin, L.; Zhang, Y.; Jing, Q.; Hou, T. C.; Wang, Z. L. Self-Powered Magnetic Sensor Based on a Triboelectric Nanogenerator. *ACS Nano* **2012**, *6*, 10378–10383.
23. Zhu, G.; Chen, J.; Liu, Y.; Bai, P.; Zhou, Y.; Jing, Q.; Pan, C.; Wang, Z. L. Linear-Grating Triboelectric Generator Based on Sliding Electrification. *Nano Lett.* **2013**, *13*, 2282–2289.
24. Wang, S.; Lin, L.; Xie, Y.; Jing, Q.; Niu, S.; Wang, Z. L. Sliding-Triboelectric Nanogenerators Based on In-Plane Charge-Separation Mechanism. *Nano Lett.* **2013**, *13*, 2226–2233.
25. Nemeth, E.; Albrecht, V.; Schubert, G.; Simon, F. Polymer Tribo-electric Charging: Dependence on Thermodynamic Surface Properties and Relative Humidity. *J. Electrostat.* **2003**, *58*, 3–16.